Belle II experiment: status and prospects

Eiasha Waheed[a,*]

[a]*High Energy Accelerator Research Organisation ,*
Tsukuba, Japan

E-mail: waheede@post.kek.jp

The Belle II experiment at the SuperKEKB e^-e^+ collider is the successor to the Belle experiment. The design luminosity is $6.5 \times 10^{35} \mathrm{cm}^{-2}\mathrm{s}^{-1}$ and it aims to record integrated luminosity of 50 fb^{-1} which is 50 times more than that of Belle. The current integrated luminosity has so far reached 213 fb^{-1} by summer 2021. Belle II aims to measure the matrix elements of Cabibbo-Kobayashi-Maskawa (CKM) matrix and their phases with unprecedented precision. With 50 fb^{-1} of data, Belle II will be able to discover new physics beyond the Standard Model. The initial physics results have already confirmed the performance of the detector. We briefly report the status and prospects of the Belle II experiment.

---

*Speaker

1. Introduction

   Flavour physics plays a crucial role in the search for physics beyond the Standard Model (SM). The decay of B meson not only offers many measurements of the fundamental parameters of the SM but also of rare decays and CP violation. Large datasets are needed for precise determination of SM parameters and to be more sensitive to possible small deviations from the SM predictions. The first generation of B factories, BaBar and Belle [1], operated for 10 years achieving substantial results. Both experiments gave significant contributions to B physics and were able to find the first evidence of the CP violation outside the kaon system and the experimental confirmation of the CKM mechanism. A second generation B-factory, characterized by low-background environment and large data samples of B, D, and τ, will give exclusive advantages to its experiment w.r.t. LHC. Belle II will be able to explore flavor physics with B meson, charmed mesons, τ leptons and quarkonium physics. Belle II has also a unique capability to search for low mass dark matter and low mass mediators. Belle II has many advantages over LHCb such as its lower backgrounds from e^+e^- collisions, its excellent ability to reconstruct the the neutral particles (π^0, γ, η). The Belle II trigger has very less bias on lifetime and kinematic properties. The missing energy and missing mass analysis are also straightforward as the initial state energy and momentum are known in Belle II.

2. SuperKEKB and Belle II detector

   SuperKEKB is an asymmetric electron-positron collider aiming at delivering the highest instantaneous luminosity ever reached ($6.5 \times 10^{35} \mathrm{cm}^{-2}\mathrm{s}^{-1}$ and to collect integrated luminosity of 50 fb^{-1}. It collides electrons with an energy of 7 GeV and positrons with an energy of 4 GeV, leading to a center of mass energy in the region of the Υ resonances. Most of the data is collected at the the $\Upsilon(4S)$ resonance that is just above the threshold for $B\bar{B}$. There are two essential elements that allow the increase of luminosity: the reduced beam size by a factor 20 and an increase in the beam currents by a factor 1.5. However with the increase in luminosity, beam backgrounds also increases.

   The Belle II detector [2] operates in a harsher environment as compared to Belle. To cope with the high beam background and to improve the Belle II detector performance than that of Belle performance, all the Belle II components have been substantially upgraded or new detectors are installed. There are some substantial changes with respect to the Belle detector that will have a relevant impact on the Belle II performance. The new tracking system, consisting of a Pixel Vertex Detector (PXD), a Silicon strip Vertex Detector (SVD) and a Central Drift Chamber (CDC) will contribute in vertex reconstruction improvements. A better charge track reconstruction and dE/dx measurement will be allowed by a larger central drift chamber. A time-of-propagation counter and the aerogel ring-imaging Cherenkov detector are used for particle identification with a fake rate lower than in Belle. The electromagnetic calorimeter, based on Belle's CsI(Tl) crystal calorimeter, but with new front-end electronics and waveform fitting algorithm, is used for electron and photon reconstruction. For the detection of K_L and muon, KL and muon detector have also been upgraded. The design choices of the Belle II detector translate into improvements on the impact parameter resolution, increase in K_s efficiency, a better K/π separation and π^0 reconstruction. The schematic

of the Belle II detector is shown in Fig. 1. Data taking at Belle II started in March 2019 and by the summer run 2021, 213.49 fb^{-1} integrated luminosity has been reached with 90% data taking efficiency.
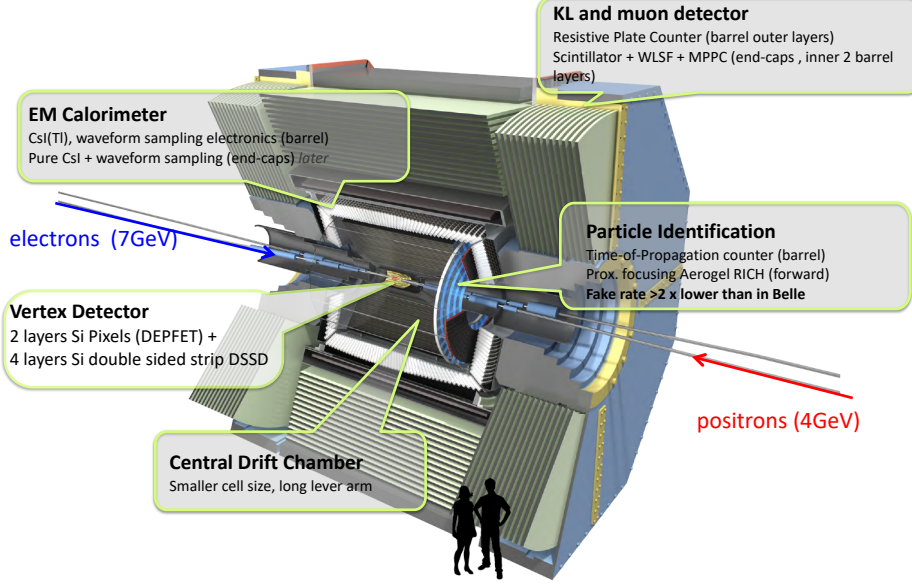

Figure 1: Schematic of the Belle II detector.

3. D^0 and D^+ **lifetime measurements**

Precise measurement of charm meson lifetime is challenging due to the contributions of strong interaction to the decay amplitudes. Apart from that it is an important ingredient to many theoretical calculations as well as experimental measurements. The lifetime measurement with early Belle II data will demonstrate the excellent vertexing capability of the Belle II detector which is essential for future analyses of decay-time-dependent measurements. Belle II reported the most precise measurements of the D^0 and D^+ lifetimes using $D^{*+} \to D^0 (\to K^- \pi^+) \pi^+$ and $D^{*+} \to D^+ (\to K^- \pi^+ \pi^+) \pi^0$ decays [4]. The D^0 and D^+ candidates are reconstructed using charged tracks identified as kaons and pions. Low momentum π^0 is reconstructed from two photons as, $\pi^0 \to \gamma \gamma$. The D^{*+} momentum in $e^+ e^-$ centre-of-mass frame is required be greater than 2.5(2.6) GeV/c to suppress $D^0 (D^+)$ mesons coming from B mesons. The mass of D^0 and D^+ candidate is required to be $1.75 < m(K^- \pi^+) < 2.0$ GeV/c^2. The difference between the D^{*+} and D candidate masses, ΔM, must satisfy $144.94 < \Delta M < 145.90$ MeV/c^2 and $138 < \Delta M < 143$ MeV/c^2 for D^0 and D^+ candidates, respectively. By applying these selections, D^0 candidates have signal purity of 99.8% in the signal region, defined as $1.851 < m(K^- \pi^+) < 1.878$ GeV/c^2. The signal region in $m(K^- \pi^+ \pi^+)$ is defined as $1.855 < m(K^- \pi^+ \pi^+) < 1.883$ GeV/c^2 with a background contamination of 9%. Mass distributions of $D^0 \to K^- \pi^+$ and $D^+ \to K^- \pi^+ \pi^+$ candidates are shown in Fig. 2.

The lifetime is extracted with a likelihood fit to the unbinned distributions of the lifetime and its uncertainty (t, σ_t). The background contribution is neglected in D^0 decay-time fits and a systematic uncertainty is assigned whereas the background is modeled using sidebands in D^+
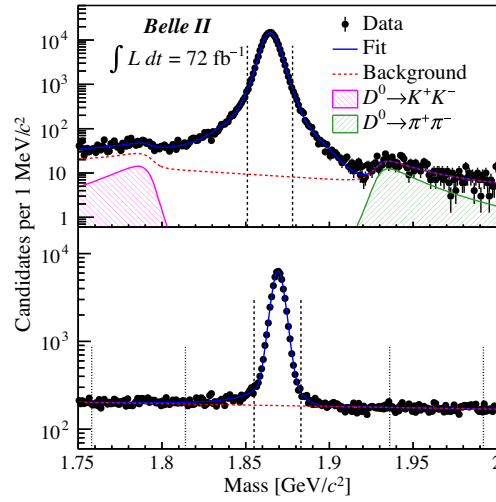
Figure 2: Mass distributions of (top) $D^0 \rightarrow K^-\pi^+$ and (bottom) $D^+ \rightarrow K^-\pi^+\pi^+$ candidates with fit projections overlaid. The vertical dashed and (for the bottom plot) dotted lines indicate the signal regions and the sideband, respectively.

decay-time fits. The decay-time distributions with fit projections are shown in Fig. 3. The results, $\tau(D^0) = 410.5 \pm 1.1(\text{stat.}) \pm 0.8(\text{syst.})$fs and $\tau(D^+) = 1030.4 \pm 4.7(\text{stat.}) \pm 3.1(\text{syst})$fs, are the world's most accurate measurements and agree with previous measurements.
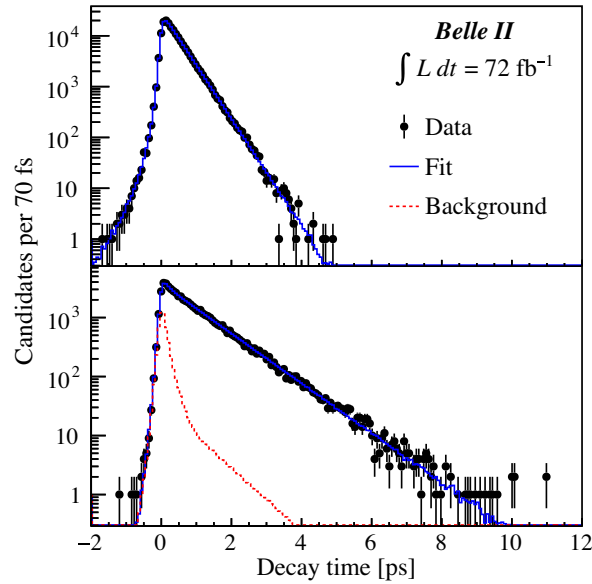

Figure 3: Decay-time distributions of (top) $D^0 \rightarrow K^-\pi^+$ and (bottom) $D^+ \rightarrow K^-\pi^+\pi^+$ candidates in their respective signal regions with fit projections overlaid.

4. $B^0 \to \pi^0\pi^0$ and $B^+ \to \rho^+\rho^0$ decays

Belle II is expected to significantly improve measurements of the CKM phase α/ϕ_2 [3, 6]. Decays of π^0 candidates are reconstructed by using two isolated clusters in the electromagnetic calorimeter, with requirements on the helicity angle and kinematic-fit quality to constrain π^0 mass. $B^+ \to \rho^+\rho^0$ is pion only final state where the main background is coming from the width of ρ mass. The measured branching ratios are shown in following equations,

$$\mathcal{B}(B^0 \to \pi^0\pi^0) = (0.98^{+0.48}_{-0.39} \pm 0.27) \times 10^{-6}, \tag{1}$$

$$\mathcal{B}(B^+ \to \rho^+\rho^0) = (20.6 \pm 3.2 \pm 4.0) \times 10^{-6}, \tag{2}$$

where the first error is statistical and the second is systematic error. These are the first reconstruction of $B^0 \to \pi^0\pi^0$ and $B^+ \to \rho^+\rho^0$ decay performed with early Belle II data that corresponds to 62.8 fb^{-1}. The results are compatible world average values.

5. ϕ_3/γ measurement with combined Belle + Belle II data

A theoretically clean measurement of the angle ϕ_3/γ can be obtained using CP-violating $B \to D^{(*)}K^{(*)}$ decays. In the BPGGSZ formalism, $b \to u\bar{c}s$ amplitude (A_{sup}) is suppressed relative to the $b \to c\bar{u}s$ amplitude (A_{fav}). The two amplitudes are related by

$$\frac{A_{\text{sup}}(B^- \to \bar{D}^0K^-)}{A_{\text{fav}}(B^- \to D^0K^-)} = r_B e^{i(\delta_B - \phi_3)}, \tag{3}$$

where r_B is the magnitude of the ratio of amplitudes and δ_B is the strong-phase difference between the favoured and suppressed amplitudes. The first combined Belle and Belle II measurement is performed for ϕ_3/γ [7]. $B^\pm \to DK^\pm$ and $B^\pm \to D\pi^\pm$ decays are reconstructed with D decays into $K^0_S\pi^-\pi^+$ final states. The main source of background events are coming from the $e^+e^- \to q\bar{q}$ ($q = u, d, s, c$) continuum process. These backgrounds are suppressed by utilizing the event topology, which is different from that of $B\bar{B}$ events, with a binary classifier based on boosted decision trees. The signal yield in each D phase-space bin is determined from a two-dimensional extended maximum-likelihood fit to ΔE and transformed FBDT output (C') simultaneously in $B \to D\pi$ and $B \to DK$. The fit distributions are shown in Fig. 4 and 5 and the results are given in Eq. 4.

$$\begin{aligned}
\phi_3 &= (78.4 \pm 11.4 \pm 0.5 \pm 1.0)^\circ, \\
r_B^{DK} &= 0.129 \pm 0.024 \pm 0.001 \pm 0.002, \\
\delta_B^{DK} &= (124.8 \pm 12.9 \pm 0.5 \pm 1.7)^\circ.
\end{aligned} \tag{4}$$

The statistical uncertainty has improved by 30% with just 20% increase in data along with improvement of experimental systematics which reduced from 4° to 0.5°. The systematics associated with the inputs also reduced from 4° to 1° due to recent updates from by BESIII [8, 9].
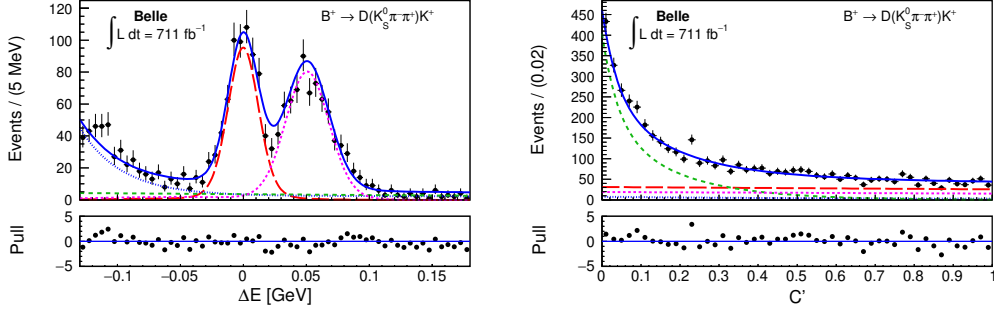
Figure 4: Distributions of (left) ΔE and (right) C' for Belle for $B^+ \to D(K_S^0 \pi^- \pi^+)K^+$ candidates restricted to the signal-enhanced region in the Belle data set with fit projections overlaid.

Figure 5: Distributions of (left) ΔE and (right) C' for Belle II for $B^+ \to D(K_S^0 \pi^- \pi^+)K^+$ candidates restricted to the signal-enhanced region in the Belle II data set with fit projections overlaid.

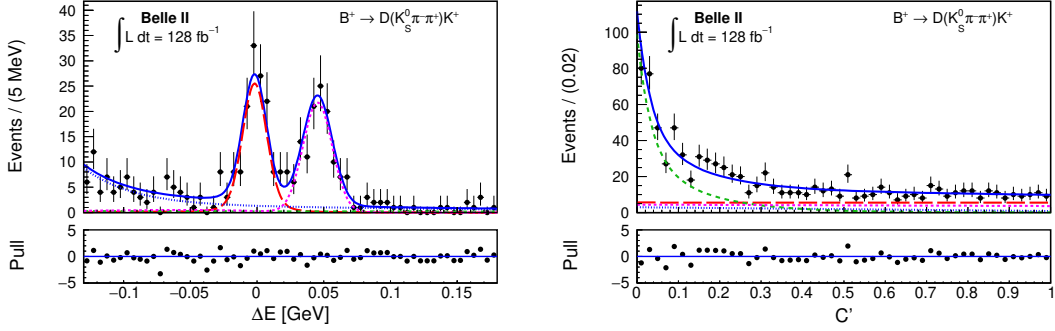## 6. $B^+ \to K^+ \ell^+ \ell^-$ and $B^+ \to K^+ \nu \bar{\nu}$ decays

The rare decays $B^+ \to K^+ \ell^+ \ell^-$ involve a $b \to s$ quark level transition and are mediated by a flavor changing neutral current. As a consequence they are forbidden at tree level and propagate through electro-weak penguin or box diagrams. These decays are highly suppressed, and are sensitive to new physics. The signal yield is determined from a two-dimensional fit to M_{bc} and ΔE which is equal to $8.6^{+4.3}_{-3.9} \pm 0.4$ events with 62.8 fb^{-1} data. The ratio of branching fraction of the muon to electron channel is a sensitive probe for new physics. More data is needed to perform a full $R_{K(*)} = \frac{\mathcal{B}(B \to K^{(*)} \mu^+ \mu^-)}{\mathcal{B}(B \to K^{(*)} \ell^+ \ell^-)} \cong 1$ measurement.

In the SM, the $B^+ \to K^+ \nu \bar{\nu}$ decay belongs to the family of the $b \to s \nu \bar{\nu}$ flavor-changing neutral-current transitions. In the specific case of the $B^+ \to K^+ \nu \bar{\nu}$ decay a branching fraction of $(4.6 \pm 0.5) \times 10^{-6}$ is predicted in the SM [10]. A measurement is performed for a search for the $B^+ \to K^+ \nu \bar{\nu}$ using novel inclusive tagging approach with 63 fb^{-1}. In this technique, the signal K candidate in each event is chosen as the reconstructed charged-particle trajectory (track) carrying the largest transverse momentum. The remaining tracks are fit to a common vertex and, together with the remaining energy deposits, make up the rest of the event (ROE). The specific features of the signal events are captured by several discriminating variables that are employed for signal identification. These discriminating variables are used to train two binary classifiers implementing the FastBDT algorithm. These BDTs are validated by comparing response in data and simulation. No statistically significant signal is observed and an upper limit of 4.1×10^{-5} on the $B^+ \to K^+ \nu \bar{\nu}$

branching ratio is set at the 90% confidence level.

7. Semileptonic B decays

7.1 Inclusive $B \to X_c \ell \nu$

Semileptonic $B \to X_c \ell \nu$ decays offer a theoretically clean avenue to determine $|V_{cb}|$. The mass moments of the hadronic system in inclusive semileptonic $B \to X_c \ell \nu$ decays can be used to measure non-perturbative QCD parameters and the CKM matrix element $|V_{cb}|$. The measurement is performed using both tagged and untagged approaches. In the untagged approach, one well identified lepton is used to measure the signal by performing the fit to lepton momentum. The branching fraction is measured to be $\mathcal{B}(B \to X_c \ell \nu) = (9.75 \pm 0.03 (\text{stat}) \pm 0.47 (\text{syst.}))\%$ with 62.8 fb^{-1} data.

7.2 Exclusive $B \to D^{(*)} \ell \nu$

$B \to D^{(*)} \ell \nu$ has been explored using both tagged and untagged approaches. In the tagged measurement, the background is almost zero. The signal is measured by performing a fit to D^* and D^0 invariant masses. The branching fraction is measured to be $\mathcal{B}(\bar{B}^0 \to D^{*+} \ell^- \bar{\nu}) = (4.51 \pm 0.41 (\text{stat}) \pm 0.27 (\text{syst.}) \pm 0.45_{\pi_s})\%$ with 34.6 fb^{-1} data. In the untagged measurement, signal is calculated using $\cos\theta_{B,Y}$ where $\theta_{B,Y}$ is the angle between B and the direction of $D^* \ell / D^0 \ell$ system. The branching fraction is measured to be $\mathcal{B}(B^- \to D^0 \ell^- \bar{\nu}) = (2.29 \pm 0.05 (\text{stat}) \pm 0.08 (\text{syst.}))\%$ with 62.8 fb^{-1} data.

8. Conclusion

The Belle II experiment covers a very broad range of physics using an excellent detector and large statistics. Belle II has been running continuously and has collected more than 200 fb^{-1} data despite the Covid-19 pandemic. The upcoming large and clean data samples of B and D mesons will allow Belle II to search for NP and the improved measurements of various SM parameters. The results reported in this note are based on the early Belle II data show Belle II performance as expected.

References

[1] A. J. Bevan *et al.* (BaBar, Belle collaboration), "The Physics of the B Factories," Eur. Phys. J. C 74, 3026 (2014).

[2] T. Abe (Belle II collaboration), arXiv: 1011.0352

[3] W. Altmannshofer *et al.* (Belle II collaboration),"The Belle II Physics Book,"PTEP **2019**,123C01 (2019).

[4] F. Abudinén *et al.*(Belle II collaboration), "Precise measurement of the D^0 and D^+ lifetimes at Belle II", Phys. Rev. Lett. **127** (2021) 211801.

[5] J. -F. Krohn *et al.* (Belle-II analysis software group), "Global Decay Chain Vertex Fitting at B-Factories", Nucl. Instrum. Meth. **A976**, 164269 (2020).

[6] M. Gronau and D. London, Phys. Rev. Lett. **65** (1990) 3381.

[7] F. Abudinen *et al.* (Belle and Belle II collaboration),"Combined analysis of Belle and Belle II data to determine the CKM angle ϕ_3 using $B^+ \rightarrow D(K_S^0 h^+ h^-)h^+$ decays ", JHEP **02** (2002) 063.

[8] BESIII collaboration, "Model-independent determination of the relative strong-phase difference between D^0 and $\bar{D}^0 \rightarrow K_{S,L}^0 \pi^+ \pi^-$ and its impact on the measurement of the CKM angle γ/ϕ_3", Phys. Rev. D **101** (2020) 112002.

[9] BESIII collaboration, "Improved model-independent determination of the relative strong-phase difference between D^0 and $\bar{D}^0 \rightarrow K_{S,L}^0 \pi^+ \pi^-$ and its impact on the measurement of the CKM angle γ/ϕ_3", Phys. Rev. D **102** (2020) 052008.

[10] T. Blake, G. Lanfranchi, and D. M. Straub. Rare B Decays as Tests of the Standard Model. Prog. Part. Nucl. Phys., 92:50–91, 2017.